Research Article

Ziyad Majeed Abed*, Wasan Ismail Khalil and Hisham Khalid Ahmed

Effect of waste tire products on some characteristics of roller-compacted concrete

https://doi.org/10.1515/eng-2022-0559 received October 11, 2023; accepted November 11, 2023

Abstract: Roller-compacted concrete pavement (RCCP) is one of the most durable, economical, and practical solutions for the construction of roads for various heavy-duty purposes. To make RCCP more sustainable, different waste materials have been utilized. These materials were densified silica fume (SF), ground granulated blast furnace slag (S), crumb rubber (CR), and recycled steel fibers (RSFs) from waste tires. The weight percentages of replacement for SF and S from cement were 5, and 27.5%, respectively. CR was utilized as a volumetric replacement of sand with 0, 2, 5, and 10%. As a volumetric addition of concrete, RSF with 0.2, 0.4, and 0.6% was utilized. Water content was 6% for all mixtures. The impact resistance test was performed to evaluate the behavior of RCCP to the repeated load on roads. Also, ultrasonic pulse velocity (UPV) (nondestructive) and abrasion resistance tests were performed to validate roller-compacted concrete (RCC) as pavement. There is a substantial increase in impact energy by using 10% of CR and 0.6% of RSF, compared with that of reference specimens. The use of CR and RSF can improve the abrasion resistance of RCC, and this can ensure its applications in pavements. The relationships between impact, abrasion, and UPV were established, and models have been proposed to predict these relationships.

Keywords: roller compacted concrete, crumb rubber, Pozzolana, impact resistance, ultrasonic pulse velocity, abrasion resistance

Wasan Ismail Khalil: Civil Engineering Department, University of Technology-Iraq, 10066, Baghdad, Iraq

Hisham Khalid Ahmed: Building and Construction Department, Technical Eng. College, Al-Esraa University, Baghdad, Iraq

1 Introduction

Roller compacted concrete (RCC) is a zero-slump concrete defined as "concrete compacted by roller compaction; concrete that, in its unhardened state, will support a roller while being compacted" by the American Concrete Institute (ACI) committee [1]. RCC might be subjected to vehicular loadings upon immediate exposure to traffic, as stated by the European Ready Mixed Concrete Organization [2]. RCC emerges as a sustainable solution for the construction and restoration of pavements owing to its low carbon emissions, durability, and low maintenance demands [3,4]. Over 300 million tires are annually subjected to disposal. Due to their nonbiodegradable nature, tires pose a challenge in terms of landfill capacity, as they occupy substantial volumes of space [5]. The presence of waste tires in junkyards can have a significant impact on the environment as they have the potential to emit noxious gases and hazardous chemicals into the surrounding air, soil, and water [6]. Approximately 66% of these tires remain untreated, leading to the formation of unauthorized waste disposal sites [7]. Hence, numerous investigations have been conducted to assess the advantages and disadvantages of crumb rubber (CR) on various characteristics of concrete. RCC pavement mixtures incorporate a cementitious material content ranging from 10 to 17% by dry weight of aggregate, equivalent to approximately 208–356 kg/m³ [8]. From previous research studies, CR, utilized with percentages 4-10% as a replacement of fine aggregate, showed results close to reference or an improvement in properties such as compressive, flexural, splitting strengths, abrasion resistance (AR), water absorption, modulus of elasticity, and durability [9–13]. Using CR instead of fine aggregates with a larger particle size (2-4 mm) enhanced the mechanical properties of the concrete more than using finer aggregates [14]. In addition, soaking CR in the NaOH solution at 10% concentration for 24 h will enhance or mitigate the degradation of rubberized concrete's physical properties. Rubberized concrete made with 24-h NaOH-treated CR had 25 and 5% higher compressive and flexural values than concrete made with untreated CR [15]. Investigation on different laboratory compaction techniques (vibratory

^{*} Corresponding author: Ziyad Majeed Abed, Civil Engineering Department, University of Technology-Iraq, 10066, Baghdad, Iraq, e-mail: 40293@uotechnology.edu.iq

2 — Ziyad Majeed Abed *et al.* DE GRUYTER

hammer, vibrating table, modified Proctor test, and Superpave gyratory compactor) affect RCC's mechanical and physical characteristics. The results demonstrated that the Superpave gyratory and vibrating hammer approaches performed effectively in strength and compaction ratio [16]. Liew and Akbar proposed that to mitigate the occurrence of the balling effect, it is advisable to maintain the volume fraction of steel fibers at 0.5%, a mass of 30 kg/m³, and an aspect ratio of 200 [17]. In the study conducted by Ali et al. [18], it was observed that the mechanical performance of twisted recycled steel fiber (TRSF) surpassed that of plain recycled steel fiber (PRSF) when incorporated into concrete. The incorporation of recycled steel fibers (RSFs) into the concrete matrix resulted in a notable enhancement of compressive, splitting, and modulus of rupture strength more than plain concrete. RSF accelerates ultrasonic pulse velocity (UPV) and rapid chloride ion penetration except at lower volume fractions (0.25-0.5%). UPV tests showed that RSF increases concrete matrix heterogeneity and porosity, notably at large volume fractions (1-2%) [19]. Also, increased utilization of rubber in concrete will reduce UPV [20]. Also, Sallam et al. found that using 10% of CR, as fine aggregate replacement in concrete, will increase the impact resistance more than higher percentages of CR replacement [21]. Alwesabi et al. utilized CR as a replacement of fine aggregate by 20%, and different combinations of micro steel (MS) and polypropylene (PP) fibers to investigate their effect on impact resistance. The samples, reinforced with 0.9% MS + 0.1% PP hybrid concrete, achieved an impressive final impact energy, which was a remarkable 10 times higher than that of plain concrete [22].

Hence, the purpose of this study is to explore the benefits of utilizing waste materials like silica fume (SF) and slag, as a weight replacement for cement, and substituting fine aggregate with treated CR. This innovative approach holds great promise for finding sustainable solutions in construction. These substitutions were used to save money and promote environmental sustainability. Pozzolana is a great solution to reduce consumed energy in the cement industry and to increase early strength development. In addition, it plays a crucial role in preserving the mechanical properties and durability of RCC, preventing any loss due to the action of CR. Moreover, RSF was employed to enhance the impact resistance of RCC and to overcome the use of CR. UPV, a nondestructive test, was employed to assess the quality of RCC. Among previous studies, no research had been done on the influence of the combination of CR and RSF from waste tires on the AR of RCC.

2 Research significance

Nonductile (brittle) materials include rigid conventional concrete and roller-compacted concrete pavement (RCCP). This reduces the energy absorption and impact resistance of concrete. This limits the use of concrete in constructions that need strong impact resistance and energy absorption like roads subjected to repetitive mechanical loads. This study investigated and analyzed the effects of the inclusion of CR and RSF from waste tires in RCCP to achieve the required properties that cover this knowledge gap. The use of treated CR as a volumetric replacement for fine aggregate and adding RSF as a volumetric addition of RCC improves pavement feasibility, sustainability, and durability.

3 Experimental procedure

3.1 Materials characteristics and mixture design

Sulfate-resisting Portland cement (SR) (CEM I-SR 3) [3,23] constituted 16% of the dry aggregate in RCCP [8]. Densified SF and ground granulated blast furnace slag (S) were partially weight replaced in SR. The optimal Taguchi design proportions for SF, S, and water content were 5, 27.5, and 6%, respectively [24]. Figure 1 shows the optimum water content (6%) calculated by the modified proctor test (method C) [25]. The physical properties of the cementitious materials are shown in Table 1, and Table 2 illustrates the chemical analysis determined by X-ray fluorescence that conformed to ASTM and ACI [26-29]. The utilization of crushed coarse aggregate with a maximum size of 19 mm and a specific gravity of 2.55 was employed to achieve a smooth surface, decrease cement consumption, minimize segregation, and enhance the cohesiveness of RCCP [30]. The fine aggregate used had a maximum size of 4.75 mm, a specific gravity of 2.6, and a fineness modulus of 2.2. The fine and coarse aggregate experience a process of washing, air drying, and subsequent separation into various sizes. These aggregates were then stored in containers and afterward gathered through a grading process based on the center line for the common area as specified by the ACI 211.3R [31], ACI 327R [30], and SCRB [32] as shown in Figure 2. The CR, as shown in Figure 3, was supplied from the Babylon factory, cleaned from textile fibers, and utilized as a volumetric partial

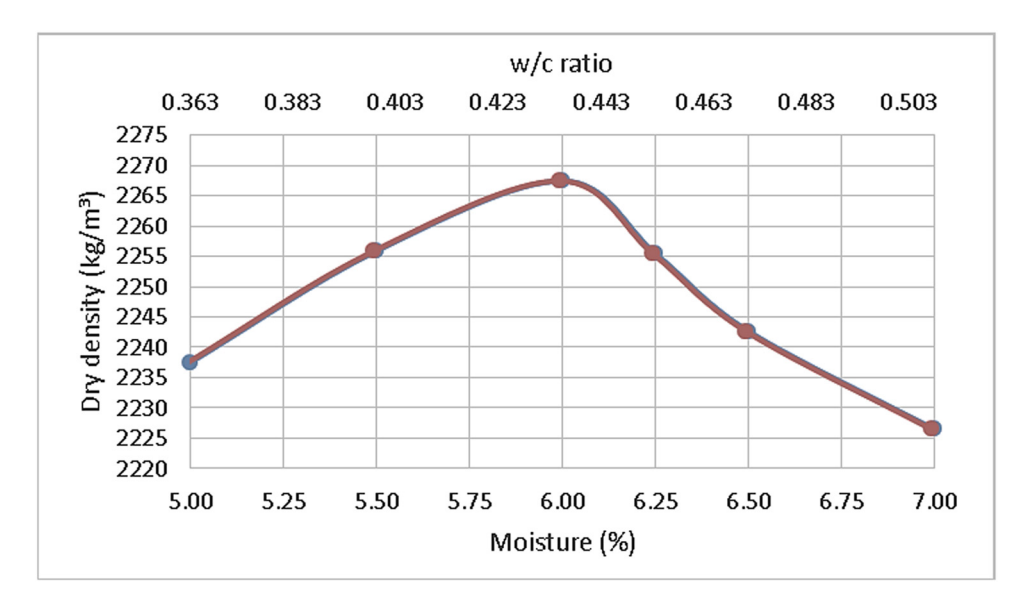


Figure 1: The optimum water content of the reference mixture.

Table 1: The physical properties of cementitious materials

Physical properties	Specific gravity	Surface area (cm²/g)	Bulk density (kg/m³)	Strength activity index (7days) (%)			
Sulfate-resisting Portland cement	3.15	3,381	1,446	_			
SF	2.24	199,960	591	114 [28]			
Ground blast furnace slag	2.9	4,181	2,901	105* [29]			

^{*}Grade 120.

Table 2: The chemical composition of cementitious materials

Oxide composition % By weight	SiO ₂	CaO	MgO	Fe ₂ O ₃	Al ₂ O ₃	SO ₃	K ₂ O	Na ₂ O	Loss on ignition	Insoluble residue
Sulfate-resisting Portland cement	22.38	62.3	2.25	4.26	3.64	2.13	0.4	0.12	2.4	0.72
Densified SF	90.7	1.6	0.7	1.1	1.3	0.09	0.31	0.2	3.4	_
Ground granulated blast furnace slag	30.3	43.1	6.9	0.97	13.52	2.95	0.55	1.225	0.2	_

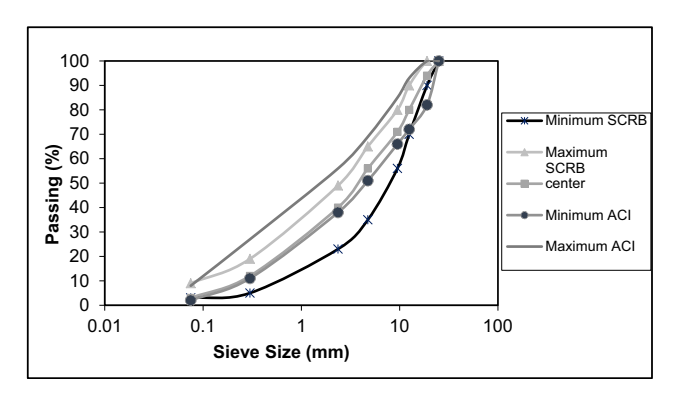


Figure 2: Grading of aggregate [3].

replacement of sand in varying proportions (0, 2, 5, and 10%). The partial percentages of CR replacement for the two sizes (0.3-2.36 mm and 2.36-4.75 mm) were about 36.4 and 63.6% of the total CR, respectively. The specific gravity and absorption of CR were 1.003 and 0.3%, respectively. Chemical treatment was employed to enhance the adhesion between the paste and CR, while also removing zinc stearate, dust, and oil. As shown in Figure 4, the treatment process involves immersing CR in a 10% concentration (2.5 M) NaOH solution for 24 h, followed by rinsing with water until neutral and subsequent drying before utilization. The chemical composition of CR is tabulated in Table 3. Three percentages of RSF were used in this study, namely,



Figure 3: Apart from utilized CR: (a) unprocessed CR and (b) processed CR.

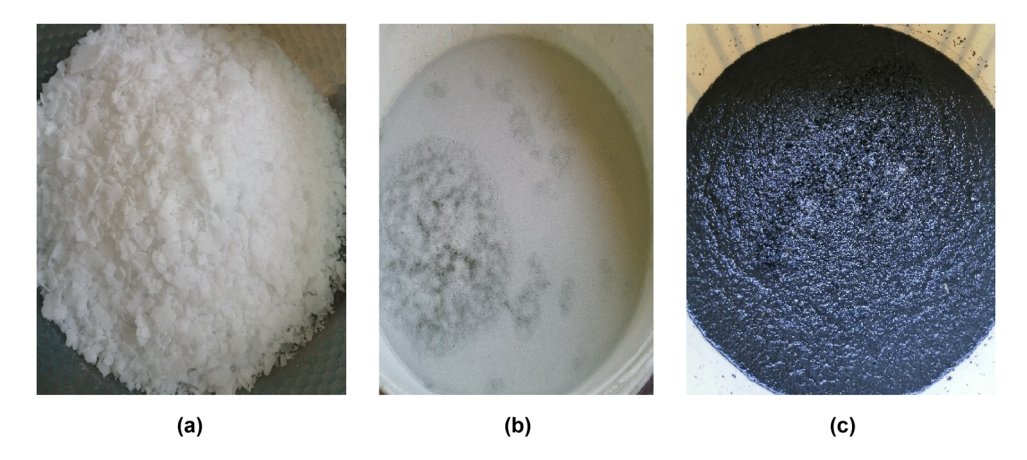


Figure 4: Treatment of CR: (a) NaOH flakes, (b) NaOH solution, and (c) CR soaked in NaOH solution.

0.2, 0.4, and 0.6% by volume of the concrete (ACI PRC-544.3) [33]. RSF was isolated and treated for contamination found in waste tires (Figure 5). RSF experienced balling as a result of increased fiber attraction beyond 0.6%. Because RSF varies geometrically, statistical analysis was employed to determine RSF lengths and diameters. For that, 500 fibers were randomly selected from recycled tire shreds. All fiber lengths and diameters were measured with 0.01 mm electronic calipers. As illustrated in Figure 6, the utilized RSF

Table 3: The chemical composition of CR*

Materials	% By weight
Hydro-carbon	48
Carbon	31
Extracted acetone	16
Ash	1.9
Residual chemical balance	3.1

^{*}From Babylon factory.

exhibited a diameter range of approximately 0.17–0.36 mm and a length range of 10–31 mm. The RSF material exhibited a tensile strength of approximately 2010 MPa, an aspect ratio (*l/d*) ranging from 60 to 85, and a specific gravity of 7.85 (conform to ACI PRC-544.3). Potable water was utilized for casting and curing of specimens in RCC mixtures. The RCC mixture proportions were determined using the guidelines provided by ACI 211.3R (Table 4). The symbolization of RCC was determined by the contents of the CR and RSF. RCC10-0.2 indicates to the RCC that has 10% CR replacement and a 0.2 of RSF.

3.2 Preparing of specimens

RCC was mixed in a lab rotary drum mixer. Coarse and fine aggregates, along with treated CR, were sequentially mixed for 1 min. Next, a uniform mixture was created by adding and thoroughly mixing the required quantities of cement, S, and SF. Water was gradually added to the mixture and





Figure 5: Apart from utilized RSF: (a) unprocessed RSF and (b) processed RSF.



Figure 6: Geometry of utilized RSF.

mixed until homogeneity was achieved. RSF was added sequentially for all the desired quantities. Cylindrical specimens of 150 \times 300 mm and 150 \times 63.5 mm were employed for UPV and drop-weight tests, respectively [34,35]. The AR test was performed on the apparatus shown in Figure 7 according to BS EN 1338 [36]. Two cubic specimens (100 mm) were cut in one of its sides to 70 mm to be its

depth. UPV tests were conducted on three specimens at ages 7, 14, and 28 days. Impact test specimens were examined using three cylinders at 28 and 56 days. Specimens were cast and compacted in oiled molds using a vibrating hammer (Figure 8), following ASTM C1435 [37]. Then, specimens were covered with a polyethylene sheet, demolded after 24 h, and cured in potable water until testing age. Specimens with various shapes utilized for impact, abrasion, and UPV tests, are illustrated in Figure 9.

4 Experimental results and discussion

4.1 Impact resistance (drop-weight test)

The drop-weight test is a common method to evaluate the effect of added materials on the energy resistance of concrete. It represents the number of blows required to make the first crack (N1) and final (failure) crack (N2).

Table 4: Proportions of RCC mixtures (kg/m³)

Mixture	Cement	SF	Slag	Fine aggregate	Coarse aggregate	CR (2.36–4.75 mm)	CR (0.30-2.36 mm)	RSF	Water	Water/ binder ratio	Sand on binder ratio
RCC0-0	228.8	16.9	93.2	1186.4	932.2	_	_	_	147.5	0.435	3.50
RCC2-0	228.8	16.9	93.2	1167.9	932.2	2.6	4.6	_	146.8	0.433	3.466
RCC5-0	228.8	16.9	93.2	1139.8	932.2	6.54	11.44	_	145.7	0.43	3.416
RCC10-0	228.8	16.9	93.2	1093.2	932.2	13.08	22.88	_	144	0.425	3.33
RCC10-0.2	228.8	16.9	93.2	1093.2	932.2	13.08	22.88	14.69	144	0.425	3.33
RCC10-0.4	228.8	16.9	93.2	1093.2	932.2	13.08	22.88	29.38	144	0.425	3.33
RCC10-0.6	228.8	16.9	93.2	1093.2	932.2	13.08	22.88	44.07	144	0.425	3.33

6 — Ziyad Majeed Abed et al. DE GRUYTER



Figure 7: Abrasion test apparatus.

Figures 10–12 illustrate the number of blows and energy resistance for first and failure cracks at the ages of 7 and 28 days, respectively. As noticed, the number of blows for first and failure cracks of RCC increased steadily as the content of CR increased. The capability of RCC for absorbing energy increases as CR increases at both first



Figure 8: Vibration hammer for compacting RCC.

stage energy $(E_{\rm I})$ and failure stage energy $(E_{\rm F})$. Energy values $E_{\rm I}$ and $E_{\rm F}$, for the mixture with 10% replacement of CR, had energy resistance higher than mixtures with 2 and 5% of CR. In the comparison of RCC10-0 to the RCC0-0, the increments for $E_{\rm I}$ were about 36.4 and 100% at ages 7 and 28 days, respectively. At the same ages, the improvement for $E_{\rm F}$ was about 42.9 and 175%, respectively. The improvement is much higher for $E_{\rm F}$ compared with $E_{\rm I}$. This is due to the low modulus of elasticity characteristics for the CR in contrast to the fine aggregate, which it partially replaced. CR contributes to bridging, flexing, twisting, and compressing RCC. This behavior makes RCC more flexible and able to absorb additional energy, as noticed in other types of concretes [38-41]. This makes it less brittle and more ductile, so it can endure greater impact without breaking. Also, CR's low modulus of elasticity reduces internal friction and recovers concrete matrix strain [42]. These results were consistent with some other researchers [43-46]. Increasing CR replacement until 10% in RCC will increase energy absorbance, and the results are identical to the results of researchers [10,47]. The ductility index was increased as the CR content increased as reported in Figure 13. This is consistent with the result of the study by Xue et al. [48]. These increments were due to the development of energy absorption at the failure stage much higher than the first crack. The impact resistance exhibited a significant improvement due to the presence of RSF in RCC through the increasing number of blows for first and failure cracks, as depicted in Figures 8-10. When compared with reference for first cracks energy at 28-day age, the percentages of increasing for RCC10-0.2, RCC10-0.4, and RCC10-0.6 were about 400, 609, and 764%, respectively. For the final crack and compared to the reference specimens, energy increased by 400, 593, and 750%, respectively. The highest percentage of increment was when adding 0.6% of RSF to the RCC. Fiber bridging over the cracks played a significant role in the enhancement of the impact resistance. When a crack tries to pass the fibers, fibers typically slow or stop crack's progression. More force is needed to overcome the fiber arrest and continue crack's propagation. As the number of fibers grows, so does the possibility of an arresting fiber [49,50]. This explains why raising the percentage of fibers to 0.2, 0.4, and 0.6% increased impact resistance and ductility [51-53]. Also, the geometry and length of RSF had a significant effect on RCC. The irregular shape of the RSF increases the impact resistance more than regular ones. At the same time, the short RSF is employed to bridge micro cracks and long RSF reduces the macro cracks [54-56]. So, RSF made RCC more ductile than reference RCC. Compared with RCC10-0 in Figure 11, the ductility index decreased

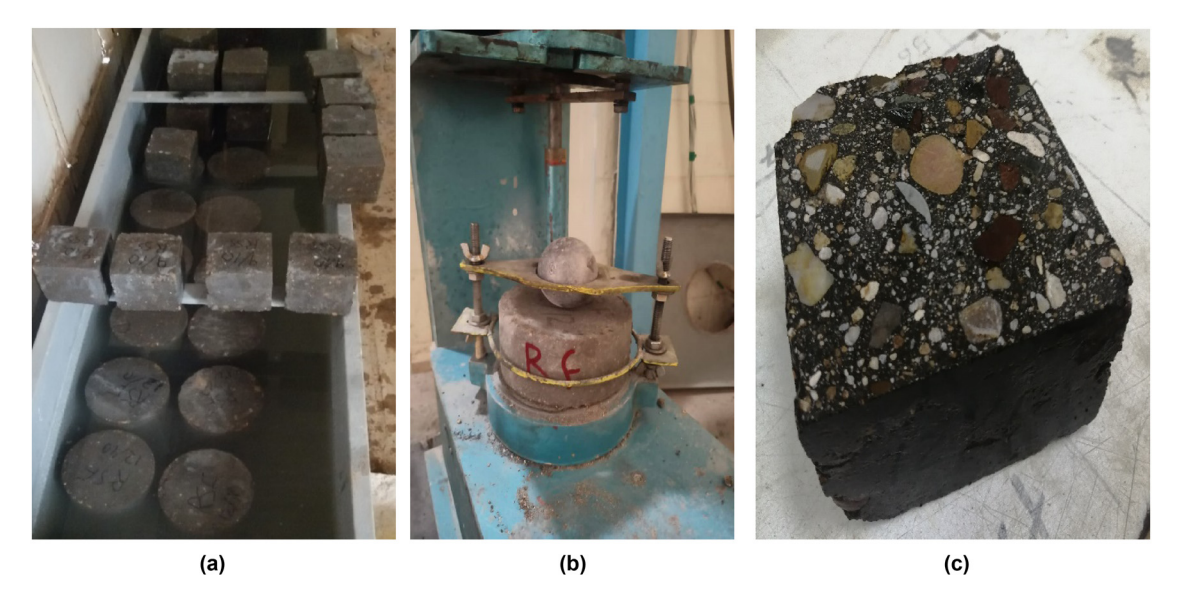


Figure 9: (a) Some specimens of tests, (b) impact test specimen, and (c) abrasion test specimen.

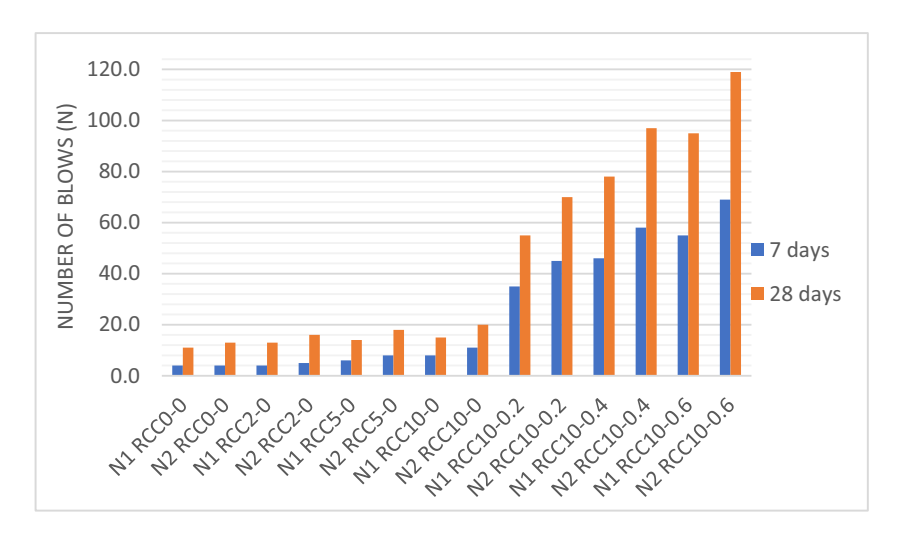


Figure 10: Number of blows for first and failure cracks of RCC.

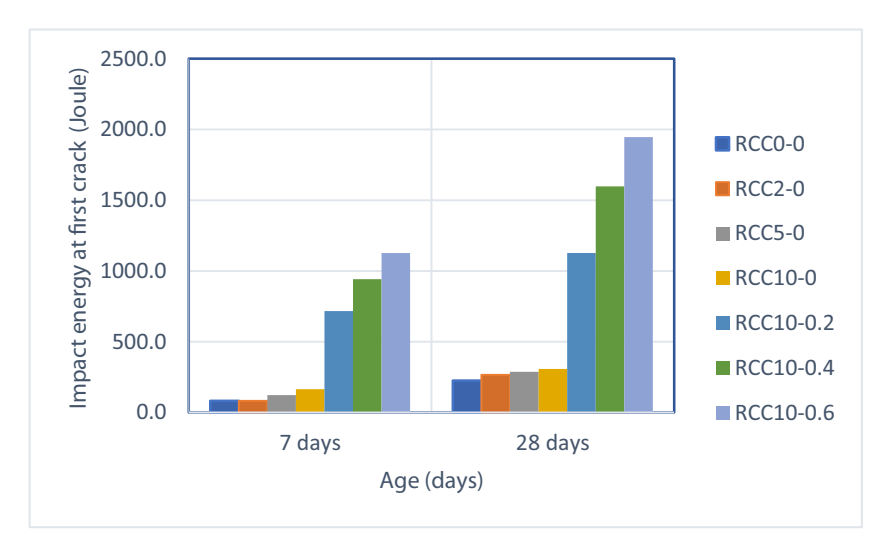


Figure 11: Impact of energy absorption at the first crack of RCC.

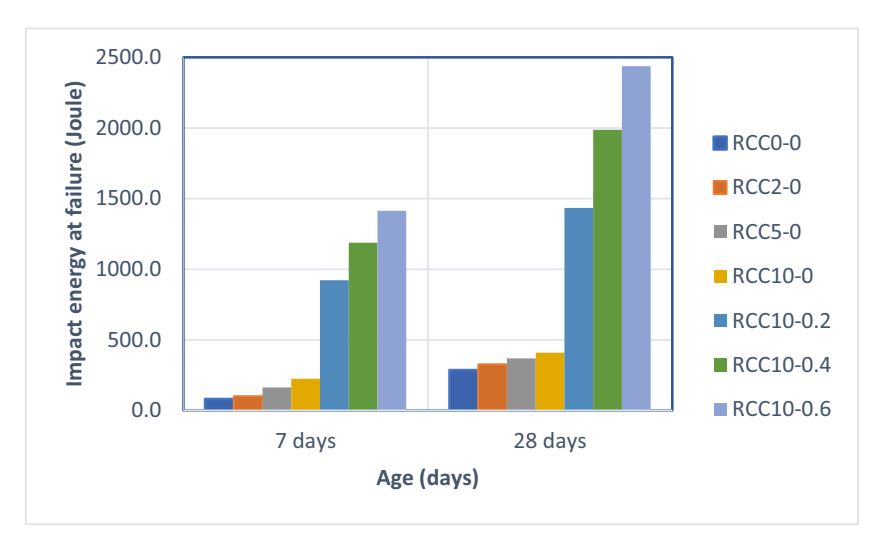


Figure 12: Impact of energy absorption at the failure crack of RCC.

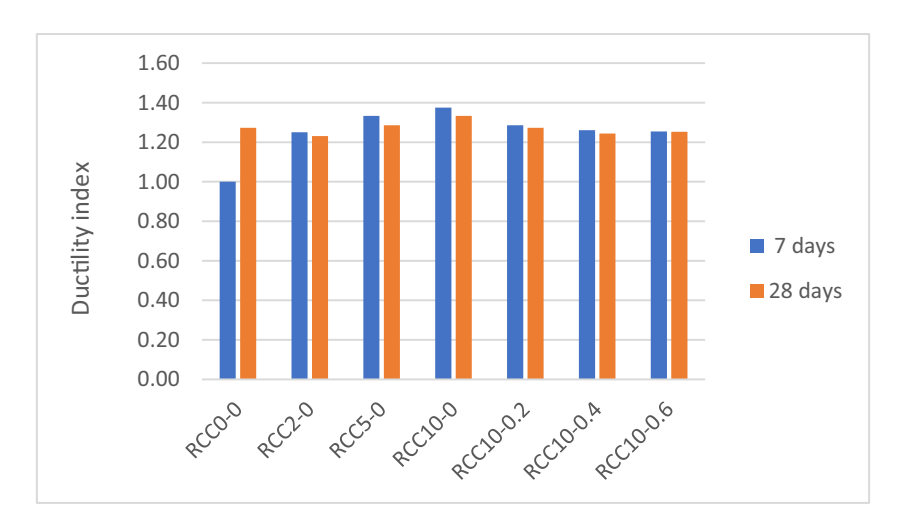


Figure 13: Ductility index of RCC mixtures.

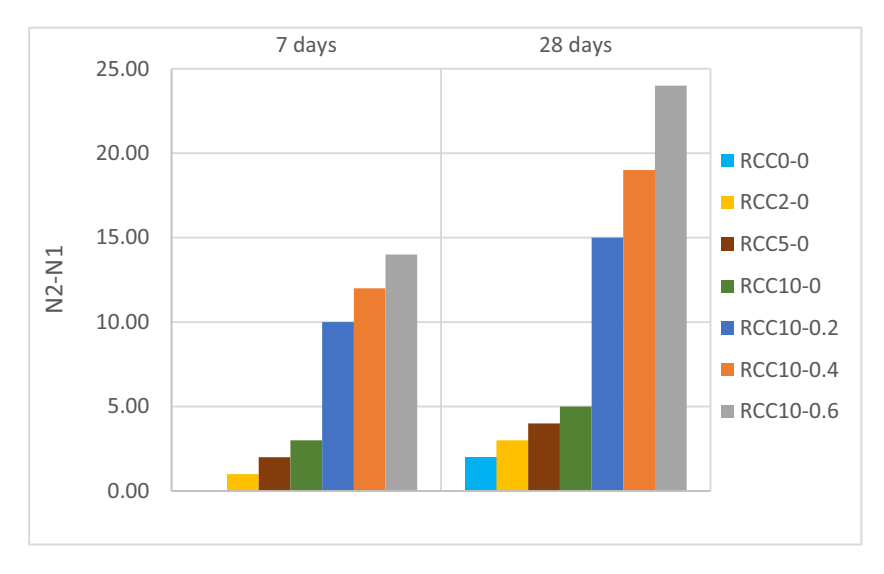


Figure 14: Difference values between N2 and N1 of RCC mixtures.

slightly as the added RSF increased. These decrements were due to the higher development of energy absorption at the first crack compared to the failure crack. Figure 14 shows the difference between the number of blows for gaining the first and final cracks. These differences increased as the energy absorption increased in RCC mixtures.

4.2 UPV

UPV is a nondestructive, dependable, and in situ test. The higher velocity value indicates an increase in the strength,

density, and homogeneity of the concrete, while the decrease in speed indicates the presence of voids, cracks, low density, and suspicious concrete. Figures 15 and 16 illustrate the effect of utilizing CR and RSF on RCC at 7, 14, and 28 days. CR contributes to a gradual downward change in UPV as the percentage of replacement increases. The velocity value experiences the most significant reduction, reaching 4.5%, when the CR replacement reaches 10% in comparison to the reference mixture, specifically at the age of 28 days [20]. At the ages of 7 and 14 days, the reduction was about 4.5, and 3.9% compared with the reference, respectively. There are some reasons for this effect. First, the UPV is

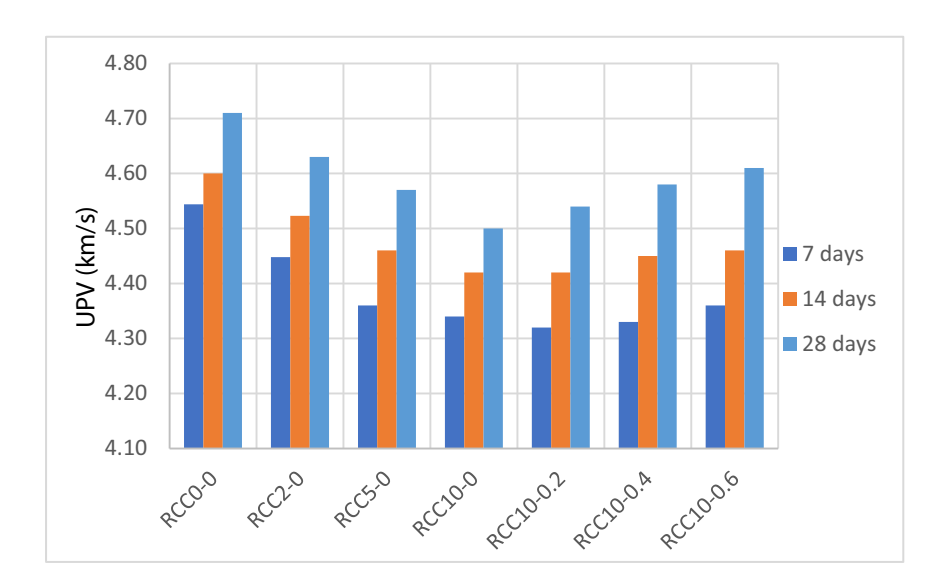


Figure 15: Effect of CR and RSF on the UPV of RCC specimens.

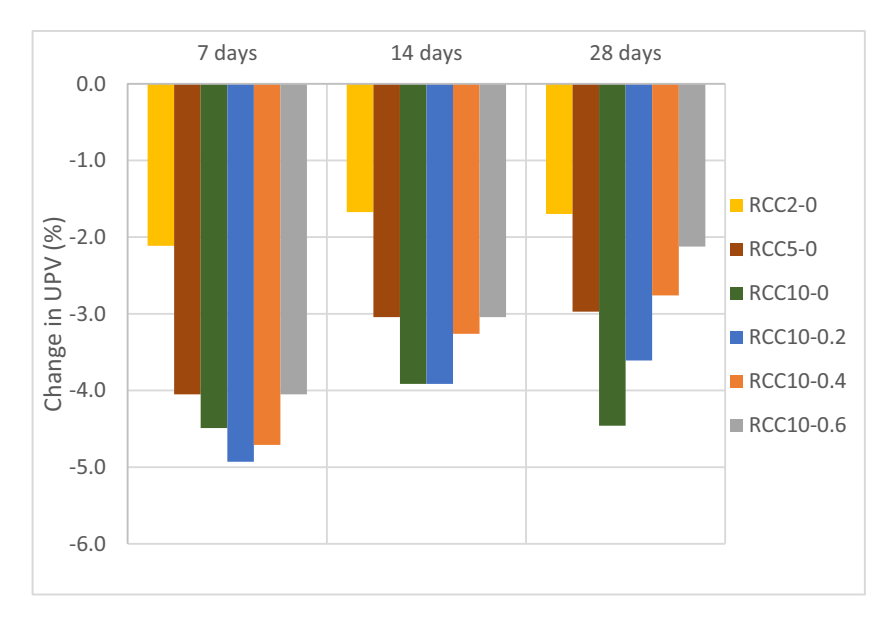


Figure 16: Change in UPV for various RCC specimens compared to the reference.

decreased by producing RCC (a rather lightweight mixture) using CR whose specific gravity is lower than that of the substituted sand. Second, the elasticity of CR facilitates the damping of compaction energy, which leads to imperfect compaction, ultimately resulting in further reduced pulse velocity. Third, CR in nature is a water-repellent material. So, the increased percentage of CR will form micro-cracks in RCC and reduce the UPV [57–59]. In a contradictory phase to the preceding statement, the utilization of RSF in RCC yielded advantageous outcomes. The application of RSF, along with constantly higher rates of addition, has resulted in a gradual enhancement of the UPV value. The addition of RSF in proportions of 0.2, 0.4, and 0.6% to the mixture RCC10-0 resulted in a corresponding rise in the UPV value at the age of 28 days with approximate increments of 1, 1.7, and 2.4%, respectively. It is undeniable that as the RSF content rises, the conductivity of the specimens develops, and with it, the UPV rises. This behavior may be because the UPV

is greater in metallic than in nonmetallic materials and the orientation of RSF [59–61]. All UPV results were above 4.5 km/s and indicate that all RCC mixtures are in excellent condition. In spite of utilizing waste materials such as CR and RSF, RCC had no significant voids or cracks that could compromise its structural stability. The increase in UPV can be assigned to the strong mechanical bond between the fibers and cementitious matrix, as well as fibers' ability to effectively prevent cracks. This results in a denser microstructure and reduced occurrence of cracks and pores in hardened RCC [62,63].

4.3 Abrasion

RCC generally has a rough texture. The coarse aggregate with a maximum size of 19 mm was employed to achieve a smooth surface. There have only been a few researches

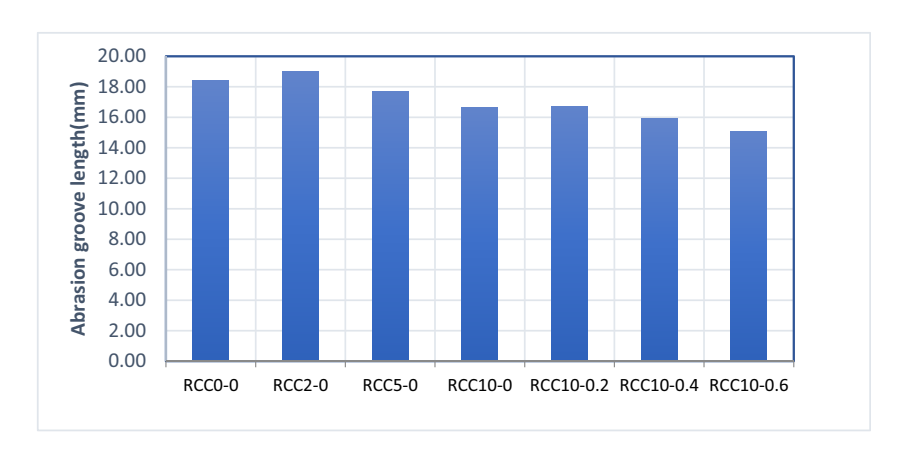


Figure 17: Abrasion groove length in the samples of RCC.

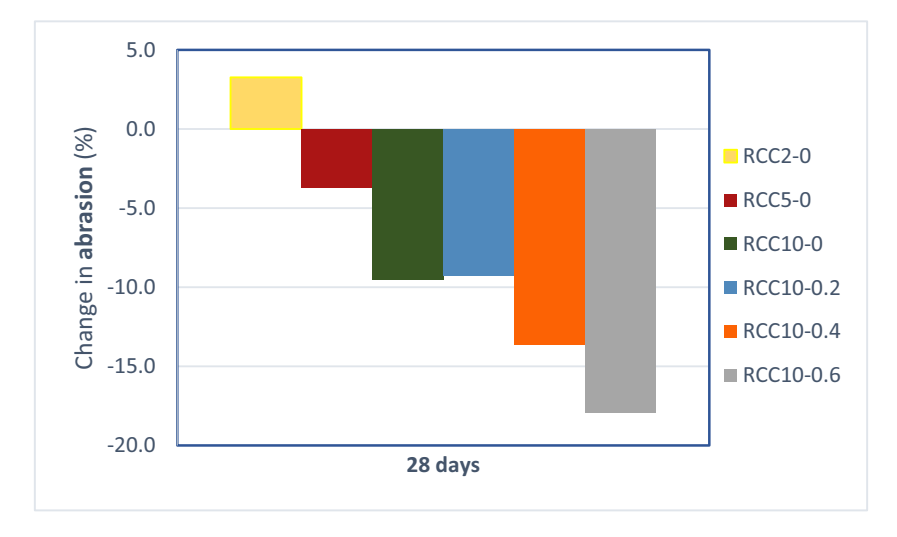


Figure 18: Change in abrasion resistance of RCC mixtures compared to RCC0-0.

done on this topic thus far. So, as shown in Figures 17 and 18, the amount of AR is slightly low when using a CR by 2%. After that, the AR begins to improve by increasing the CR content gradually, reaching a replacement percentage of 10%. At 10%, the abrasion groove length is minimal and less than that for the reference mixture by about 9.5%. This result is identical to the result obtained by Mohammed and Adamu [13] and Gesoğlu et al. [64] for other types of concrete. The reason for the improvement, in AR at 10% CR, is that CR will work as a brush on the RCC surface. This will reduce scratching and grinding on the RCC surface [65]. Also, utilizing S and SF will improve the compressive strength of concrete and increase AR [66]. The AR increases marginally with a percentage of 0.2% RSF compared to RCC10-0. After that, the AR developed as the percentage of RSF increased up to 0.6%. In comparison to 0.6% RSF addition, the AR increases to about 8.4 and 17.9% compared to the RCC10-0, and RCC0-0, respectively. This behavior is consistent with what was observed in previous research studies that studied the effect of steel fibers on other types of concrete [67-70]. Fibers prohibit cracks from spreading in RCC. It also makes the pastes stronger and more resistant to damage from abrasion. Increased hydration from the Pozzolanic reaction

increases the bond between RSF and pastes, and age leads to increased AR strength [71]. The incorporation of RSF within the RCC matrix serves as a protective layer, effectively mitigating the detrimental effects of abrasion on the surface of RCC [72,73].

4.4 Scanning electron microscopy (SEM) Analysis

To learn more about how the microstructure of RCC, utilized CR, and RSF, changed over time. SEM was performed as a testing method that uses an electron beam for scanning a sample and providing a magnified image for further study. Figure 19(a) depicts the effective pore densification and bonding of the aggregate paste in RCCO-0, which consisted of the SF and S with Pozzolanic reaction products. The fact that the hydrates successfully developed a robust connection with the aggregates is consistent with the reported peak UPV, which is an indication of high compressive strength for this specimen. But there were signs of unreacted slag particles and microscopic fissures and

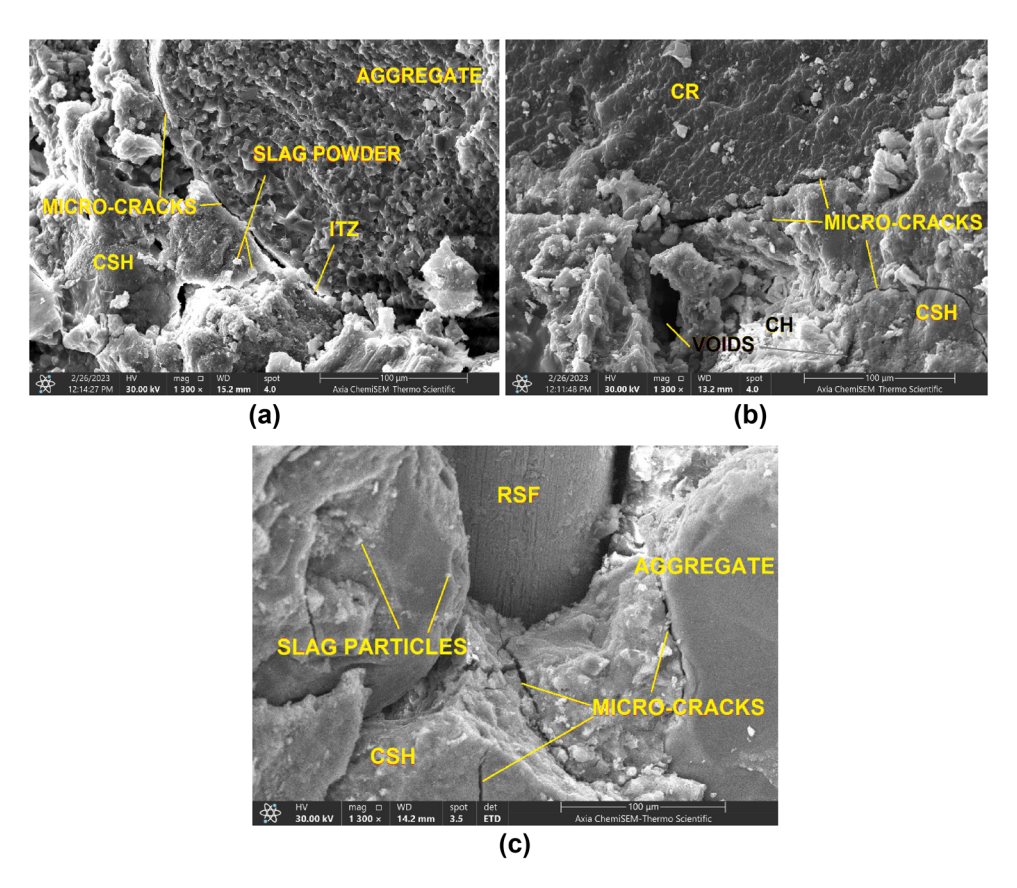


Figure 19: SEM images at 28 days. (a) Reference RCC, (b) RCC with CR, and (c) RCC with RSF and CR.

holes. The microstructure analysis of RCC including CR, as illustrated in Figure 19(b), shows that compared to natural sand, the mixture containing CR had fewer and smaller micro-cracks. Impact resistance, especially in the first crack, enhanced as CR increased. Figure 19(c) shows that the bridging action of RSF within the voids of the matrix is responsible for the increased impact resistance found in RSF-reinforced mixtures as compared to their unreinforced counterparts. Incorporating RSF, however, allowed for the discovery of numerous micro-cracks in the fibers' vicinity. This finding provides the direct proof that fiber reinforcement plays a role in reducing micro-cracks and increasing UPV values compared to un-reinforced specimen.

4.5 Relations between impact resistance, AR, and UPV

Correlations were made to determine the relationship between impact resistance and AR with UPV at 28 days of age. As shown in Figures 20 and 21, correlations were made by separating the results of mixtures with different CR contents from those with 10% CR and different RSF contents to obtain precise conclusions. It can be observed that the UPV of RCC containing CR increased as the final impact energy ($E_{\rm F\ CR}$) decreased slightly. So, the best-fit lines representing the relationship between $E_{\rm F\ CR}$ and UPV, with R^2 equal to 0.9958, are given as follows

$$E_{\rm F} = -684.34 \text{UPV} + 3492.9.$$
 (1)

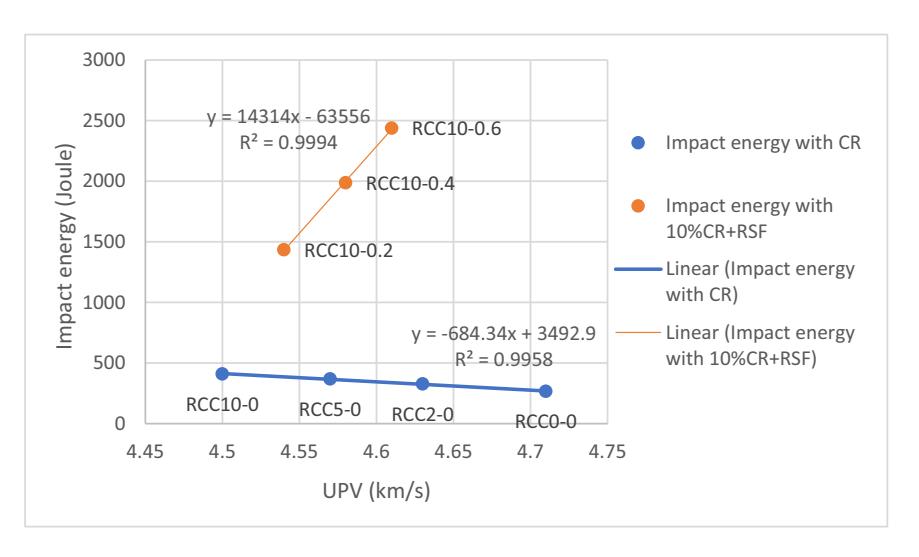


Figure 20: Relation between impact resistance and UPV of RCC at 28 days.

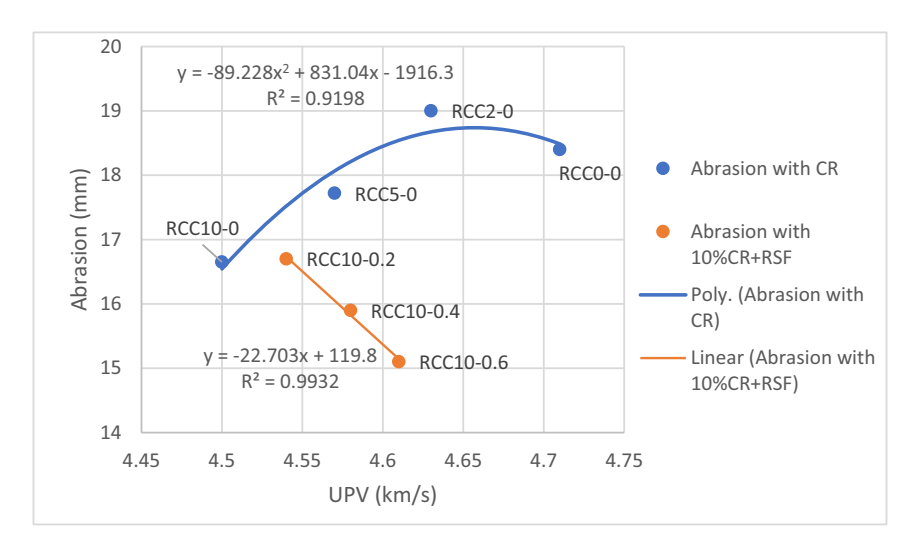


Figure 21: Relation between abrasion resistance and UPV of RCC at 28 days.

Also, Figure 20 indicates that the final impact energy improves with the increase in the RSF content, which consequently increases the UPV. A high correlation is obtained between UPV and impact energy of RCC specimens reinforced with RSF ($E_{\rm F,RSF}$) with R^2 of 0.9994. The best relation obtained to represent the fit lines is shown in equation (2):

$$E_{\rm F-RSF} = 14314 \text{UPV} - 63556.$$
 (2)

From Figure 21, it can be observed that as the CR content increases, the UPV of RCC decreases as the AR decreases and then improves in a parabolic shape. So, the best fit describes the relationship between AR and UPV is a second-degree line with R^2 of 0.9198 as follows:

$$AR_{CR} = -89.228UPV^2 + 831.04UPV - 1916.3.$$
 (3)

As a modification process, the increase in RSF content added to RCC improves the AR and hence increases the UPV. The coefficient of determination (R^2) between UPV and AR is 0.9932. The best relation obtained to represent the fit lines is shown in equation (4):

$$AR_{RSF} = -22.703UPV + 119.8.$$
 (4)

5 Conclusions

From the experimental results obtained in this study, the following conclusions can be drawn:

- 1. When the fine aggregate is replaced with CR, RCC's impact resistance increases marginally. The addition of RSF to RCC results in an extraordinary increase in energy absorption. As a result, RCC is more resistant to crack initiation under repeated impact loads.
- 2. For the UPV test, increasing the CR content in RCC decreases the value of UPV gradually. As the percentage addition of RSF increases to 0.6%, the UPV for RCC improves by about 2.4% at the age of 28 days.
- 3. Utilizing CR and RSF in RCC mixtures has a positive effect on the enhancement of AR. They improved about 9.5 and 8.4% for utilizing 10% of CR and 0.6% of RSF, respectively.
- 4. The combination of CR and RSF brings a significant positive effect on the properties and durability of RCC.
- 5. SEM images illustrate the good bond between the aggregate and paste in reference RCC, the fewer and smaller micro-cracks like the first crack in the RCC mixture containing CR, and the bridging action of RSF within the voids of the matrix, which increased the impact resistance in RSF-reinforced mixtures.
- 6. For RCC utilized CR and RSF, good correlations are obtained between UPV, impact resistance, and abrasion at 28 days of age.

Funding information: Authors declare that the manuscript was done depending on the personal effort of the author, and there is no funding effort from any side or organization.

Conflict of interest: The authors state no conflict of interest.

Data availability statement: Most datasets generated and analyzed in this study are comprised in this submitted manuscript. The other datasets are available on reasonable request from the corresponding author with the attached

References

- ACI CT-20. CT-20: ACI concrete terminology. Am Concr Inst. 2020;54.
- European Ready Mixed Concrete Organization (ERMCO). Guide to roller compacted concrete for pavements. Belgium: ERMCO publications; 2013.
- Abed ZM, Salih AA. Effect of using lightweight aggregate on [3] properties of roller-compacted concrete. ACI Mater J. 2017;114(4):517-25.
- Fardin HE, dos Santos AG. Roller compacted concrete with recycled concrete aggregate for paving bases. Sustain. 2020;12(8):1-16.
- [5] ReRubber LLC. Environmental impact of scrap tires. USA; 2022.
- EcoGreen LLC. Environmental impacts of waste tire disposal [Internet]. North Salt Lake, USA. 2021. https://ecogreenequipment. com/environmental-impacts-of-waste-tire-disposal/.
- Karaağaç B, Ercan Kalkan M, Deniz V. End of life tyre management: Turkey case. J Mater Cycles Waste Manag. 2017;19(1):577-84.
- [8] ACI PRC-325.10R. State-of-the-art report on roller-compacted concrete pavements. Am Concr Inst. 2001.
- ۲**9**1 Bisht K. Ramana PV. Waste to resource conversion of crumb rubber for production of sulphuric acid resistant concrete. Constr Build Mater. 2019 Jan 10;194:276-86.
- Fakhri M, Amoosoltani E. The effect of reclaimed asphalt pavement and crumb rubber on mechanical properties of roller compacted concrete pavement. Constr Build Mater. 2017;137:470-84.
- Liu H, Wang X, Jiao Y, Sha T. Experimental investigation of the [11] mechanical and durability properties of crumb rubber concrete. Mater (Basel). 2016;9(3):1-12.
- [12] Fakhri M, Saberik F. The effect of waste rubber particles and silica fume on the mechanical properties of Roller Compacted Concrete Pavement. J Clean Prod. 2016 Aug;129:521-30.
- Mohammed BS, Adamu M. Mechanical performance of roller [13] compacted concrete pavement containing crumb rubber and nano silica. Constr Build Mater. 2018;159:234-51.
- Gesoğlu M, Güneyisi E, Khoshnaw G, Ipek S. Investigating properties of pervious concretes containing waste tire rubbers. Constr Build Mater. 2014 Jul;63:206-13.
- Mohammadi I, Khabbaz H, Vessalas K, Enhancing mechanical per-[15] formance of rubberised concrete pavements with sodium hydroxide treatment. Mater Struct. 2016;49(3):813-27.
- Γ161 Şengün E, Alam B, Shabani R, Yaman IO. The effects of compaction methods and mix parameters on the properties of roller compacted concrete mixtures. Constr Build Mater. 2019 Dec;228:116807.

- [17] Liew KM, Akbar A. The recent progress of recycled steel fiber reinforced concrete. Constr Build Mater. 2020 Jan;232:117232.
- [18] Ali B, Farooq MA, Kurda R, Alyousef R, Noman M, Alabduljabbar H. Effect of type and volume fraction of recycled-tire steel fiber on durability and mechanical properties of concrete. Eur J Env Civ Eng. 2023;27(5):1919–40.
- [19] Mo KH, Yap SP, Alengaram UJ, Jumaat MZ, Bu CH. Impact resistance of hybrid fibre-reinforced oil palm shell concrete. Constr Build Mater. 2014 Jan 15;50:499–507.
- [20] Choi Y, Kim IH, Lim HJ, Cho CG. Investigation of strength properties for concrete containing fine-rubber particles using UPV. Mater (Basel, Switz). 2022 May;15(10):1–12.
- [21] Sallam HEM, Sherbini AS, Seleem MH, Balaha MM. Impact resistance of rubberized concrete. Eng Res J. 2008;31(3):265–71.
- [22] Alwesabi EA, Abu Bakar BH, Alshaikh IMH, Akil HM. Impact resistance of plain and rubberized concrete containing steel and polypropylene hybrid fiber. Mater Today Commun. 2020 Dec 1:25:101640.
- [23] BS EN 197-1. Cement. Composition, specifications and conformity criteria for common cements. UK: British Standards Institution; 2011.
- [24] Abed ZM, Ahmed HK, Khalil WI. Optimization of silica fume and slag in roller compacted concrete by taguchi method. Eng Technol J. 2023;41(5):724–33.
- [25] ASTM D1557. Standard test methods for laboratory compaction characteristics of soil using modified effort (56,000 ft-lbf/ft3 (2,700 kN-m/m3)). West Conshohocken, USA: ASTM International; 2012.
- [26] ASTM C150. Standard specification for portland cement. West Conshohocken, USA: ASTM International; 2014.
- [27] ACI PRC-234. Guide for the use of silica fume in concrete. USA: American Concrete Institute; 2006.
- [28] ASTM C1240. Standard specification for silica fume used in cementitious mixtures. West Conshohocken, USA: ASTM International: 2020.
- [29] ASTM C989/C989M-22. Standard specification for slag cement for use in concrete and mortars. West Conshohocken, USA: ASTM International; 2022.
- [30] ACI PRC-327. Guide to roller compacted concrete pavements. USA: American Concrete Institute: 2014.
- [31] ACI PRC-211.3R. Guide for selecting proportions for no-slump concrete. USA: American Concrete Institute; 2009.
- [32] SCRB. Standard specification for roads and bridges. Ministry of Housing and construction. Baghdad: State commission of roads and bridges; 2003.
- [33] ACI PRC-544.3. Guide for specifying, proportioning, and production of fiber-reinforced concrete. USA: American Concrete Institute; 2008.
- [34] ASTM C597. Standard standard test method for pulse velocity through concrete. West Conshohocken, USA: ASTM International; 2009.
- [35] ACI 544.2R. Measurement of properties of fiber reinforced concrete. USA: American Concrete Institute; 1999.
- [36] BS EN 1338. Concrete paving blocks- Requirements and test methods. 2003.
- [37] ASTM C1435. Standard practice for molding roller-compacted concrete in cylinder molds using a vibrating hammer. West Conshohocken, USA: ASTM International; 2014.
- [38] Schrader EK. Impact resistance and test procedure for concrete. ACI J Proc 78(2).

- [39] Kardos AJ, Durham SA. Strength, durability, and environmental properties of concrete utilizing recycled tire particles for pavement applications. Constr Build Mater. 2015 Nov;98:832–45.
- [40] Senevirathne P, Kulathunga D, Kuruwitaarachchi V. Energy absorption capacity and impact energy of rubberized concreteIn:
 13th International Research Conference. Sri Lanka: 2020. p. 87–92.
- [41] Gupta T, Sharma RK, Chaudhary S. Impact resistance of concrete containing waste rubber fiber and silica fume. Int J Impact Eng. 2015 Sep 1;83:76–87.
- [42] Khaloo AR, Dehestani M, Rahmatabadi P. Mechanical properties of concrete containing a high volume of tire–rubber particles. Waste Manaq. 2008;28(12):2472–82.
- [43] Issa CA, Salem G. Utilization of recycled crumb rubber as fine aggregates in concrete mix design. Constr Build Mater. 2013;42:48–52.
- [44] Shu X, Huang B. Recycling of waste tire rubber in asphalt and portland cement concrete: An overview. Constr Build Mater. 2014 Sep 30;67(PART B):217–24.
- [45] Mohammed BS, Awang AB, Wong SS, Nhavene CP. Properties of nano silica modified rubbercrete. J Clean Prod. 2016;119:66–75.
- [46] Adamu M, Mohammed BS, Liew MS, Alaloul WS. Evaluating the impact resistance of roller compacted concrete containing crumb rubber and nanosilica using response surface methodology and Weibull distribution. World J Eng. 2019;16:33–43.
- [47] Li HL, Xu Y, Chen PY, Ge JJ, Wu F. Impact energy consumption of high-volume rubber concrete with silica fume. Memon SA, editor. Adv Civ Enq. 2019;2019:1728762. doi: 10.1155/2019/1728762.
- [48] Xue G, Liu JX, Cao ML. A study of the impact resistance of rubber concrete at low temperatures (-30°C). Shahria Alam M, editor. Adv Civ Eng. 2019;2019:4049858. doi: 10.1155/2019/4049858.
- [49] Sukontasukkul P, Chaisakulkiet U, Jamsawang P, Horpibulsuk S, Jaturapitakkul C, Chindaprasirt P. Case investigation on application of steel fibers in roller compacted concrete pavement in Thailand. Case Stud Constr Mater. 2019;11.
- [50] Murali G, Abid SR, Amran M, Vatin NI, Fediuk R. Drop weight impact test on prepacked aggregate fibrous concrete — an experimental study. Mater (Basel). 2022;15(9):1–27. https://www.mdpi.com/1996-1944/15/9/3096.
- [51] Jia YD, Zhou ZW, Qu YD, Tian AS. Experimental research on the fracture properties of roller compacted steel fiber recycled concrete. Adv Mater Res. 2011;299–300:135–8. https://www.scopus. com/inward/record.uri?eid=2-s2.0-80052058455&doi=10.4028% 2Fwww.scientific.net%2FAMR.299-300.135&partnerID=40&md5= 8f3d259c7b26f2521f31de4210980b71.
- [52] Murali G, Santhi AS, Ganesh GM. Impact resistance and strength reliability of fiber-reinforced concrete in bending under drop weight impact load. Int J Technol. 2014;5(2):111–20. http://ijtech. eng.ui.ac.id/old/index.php/journal/article/view/403.
- [53] Abid SR, Gunasekaran M, Ali SH, Kadhum AL, Al-Gasham TS, Fediuk R, et al. Impact performance of steel fiber-reinforced selfcompacting concrete against repeated drop weight impact. Crystals. 2021;11(2). https://www.mdpi.com/2073-4352/11/2/91.
- [54] Başsürücü M, Fenerli C, Kina C, Akbaş ŞD. Effect of fiber type, shape and volume fraction on mechanical and flexural properties of concrete. J Sustain Constr Mater Technol. 2022;7(3):158–71.
- [55] Yu R, Spiesz P, Brouwers HJH. Development of ultra-high performance fibre reinforced concrete (UHPFRC): Towards an efficient utilization of binders and fibres. Constr Build Mater. 2015 Mar 15;79:273–82.
- [56] Zhang L, Zhao J, Fan C, Wang Z. Effect of surface shape and content of steel fiber on mechanical properties of concrete. Adv Civ Eng. 2020;2020:1–11.

- [57] Mohammed BS, Azmi NJ, Abdullahi M. Evaluation of rubbercrete based on ultrasonic pulse velocity and rebound hammer tests. Constr Build Mater. 2011 Mar 1;25(3):1388-97.
- [58] Marie I. Zones of weakness of rubberized concrete behavior using the UPV. J Clean Prod. 2016;116:217-22. https://www.sciencedirect. com/science/article/pii/S0959652615019216.
- [59] AL-Ridha ASD, Abbood AA, Al-Chalabi SF, Aziz AM, Dheyab LS. A comparative study between the effect of steel fiber on ultrasonic pulse velocity (UPV) in light and normal weight self-compacting concretes. In: ICCEET; 2020. IOP Conf. Series: Materials Science and
- [60] Gebretsadik BT. Ultrasonic pulse velocity investigation of steel fiber reinforced self-compacted concrete. Master's Thesis. University of Nevada: 2013.
- [61] Perumal R, Nagamani K. Impact characteristics of high-performance steel fiber reinforced concrete under repeated dynamic loading. Int J Civ Eng. 2014 Dec 10;12(4):513-20. [cited 2023 Aug 23]. http://ijce.iust.ac.ir/article-1-872-en.html.
- [62] Aslani F, Nejadi S. Bond characteristics of steel fiber and deformed reinforcing steel bar embedded in steel fiber reinforced self-compacting concrete (SFRSCC). Open Eng. 2012;2(3):445-70. doi: 10. 2478/s13531-012-0015-3.
- [63] ACI Committee 549R. Report on Ferrocement. 2009.
- [64] Gesoğlu M, Güneyisi E, Khoshnaw G, Ipek S. Abrasion and freezing-thawing resistance of pervious concretes containing waste rubbers. Constr Build Mater. 2014 Dec;73:19-24.
- [65] Thomas BS, Kumar S, Mehra P, Gupta RC, Joseph M, Csetenyi LJ. Abrasion resistance of sustainable green concrete containing

- waste tire rubber particles. Constr Build Mater. 2016 Oct 15:124:906-9.
- [66] Kang J, Zhang B, Li G. The abrasion-resistance investigation of rubberized concrete. J Wuhan Univ Technol Sci Ed. 2012;27(6):1144-8. doi: 10.1007/s11595-012-0619-8.
- [67] Yavuz Bayraktar O, Kaplan G, Shi J, Benli A, Bodur B, Turkoglu M. The effect of steel fiber aspect-ratio and content on the fresh, flexural, and mechanical performance of concrete made with recycled fine aggregate. Constr Build Mater. 2023 Mar 3;368:130497.
- [68] Ayoob NS, Abid SR, Hilo AN, Daek YH. Water-impact abrasion of self-compacting concrete. Mag Civ Eng. 2020;96(4):60-9.
- [69] Wu F, Yu Q, Chen X. Effects of steel fibre type and dosage on abrasion resistance of concrete against debris flow. Cem Concr Compos. 2022 Nov 1:134:104776.
- [70] Deng Q, Zhang R, Liu C, Duan Z, Xiao J. Influence of fiber properties on abrasion resistance of recycled aggregate concrete: Length, volume fraction, and types of fibers. Constr Build Mater. 2023 Jan 2;362:129750.
- [71] Wang L, Zhou SH, Shi Y, Tang SW, Chen E. Effect of silica fume and PVA fiber on the abrasion resistance and volume stability of concrete. Compos Part B Eng. 2017 Dec 1;130:28-37.
- [72] Liu YW, Lin YY, Cho SW. Abrasion behavior of steel-fiber-reinforced concrete in hydraulic structures. Appl Sci. 2020 Aug 11;10(16):5562. [cited 2023 Sep 18]. https://www.mdpi.com/2076-3417/10/16/5562.
- [73] Muhammed AJ, Qasim ZI, Al-Rubaee RH. Modifying the Properties of Open-Graded Friction Course by Adding Cellulose Fiber. Eng Technol J. 2022;40(11):1365-75. https://etj.uotechnology.edu.iq/ article_174874.html.